# Experimentally Induced Metamorphosis in Axolotl *(Ambystoma mexicanum)* Under Constant Diet Restructures Microbiota Accompanied by Reduced Limb Regenerative Capacity

**Turan Demircan[1,6*], Guvanch Ovezmyradov[2,6] , Berna Yıldırım[6], İlknur Keskin[3,6], Ayşe Elif İlhan[6], Ece Cana Fesçioğlu[6], Gürkan Öztürk[4,6], Süleyman Yıldırım [5,6*]**

[1]Department of Medical Biology, International School of Medicine, İstanbul Medipol University, Istanbul, Turkey.

[2]Department of Biostatistics and Medical Informatics, International School of Medicine, Istanbul Medipol University, Istanbul, Turkey.

[3]Department of Histology and Embryology, School of Medicine, Istanbul Medipol University, Istanbul, Turkey.

[4]Department of Physiology, International School of Medicine, İstanbul Medipol University, Istanbul, Turkey.

[5]Department of Microbiology, International School of Medicine, İstanbul Medipol University, Istanbul, Turkey.

[6]Regenerative and Restorative Medicine Research Center, REMER, İstanbul Medipol University, Istanbul, Turkey.

*To whom correspondence may be addressed:

Süleyman Yıldırım. PhD
Istanbul Medipol University, International School of Medicine, Kavacik, Istanbul, Turkey. Tel: +90-216-681-5100, Fax: +90-212-531-7555,

E-mail: suleymanyildirim@medipol.edu.tr

Turan Demircan, PhD,
Istanbul Medipol University, International School of Medicine, Kavacik, Istanbul, Turkey. Tel: +90-216-681-5100, Fax: +90-212-531-7555,

E-mail: tdemircan@medipol.edu.tr

## Abstract

Axolotl (*Ambystoma mexicanum*) is a critically endangered salamander species and a model organism for regenerative and developmental biology. Despite life-long neoteny in nature and in captive-bred colonies, metamorphosis of these animals can be experimentally induced by administering Thyroid hormones (THs). However, biological consequences of this experimental procedure, such as host microbiota response and implications for regenerative capacity, remain largely unknown. Here, we systematically compared host bacterial microbiota associated with skin, stomach, gut tissues and fecal samples based on 16S rRNA gene sequences, along with limb regenerative capacity, between neotenic and metamorphic Axolotls. Our results show that distinct bacterial communities inhabit individual organs of Axolotl and undergo substantial restructuring through metamorphosis. Drastic restructuring was observed for skin microbiota, highlighted by a major transition from *Firmicutes*-enriched to *Proteobacteria*-enriched relative abundance and precipitously decreased diversity. Remarkably, shifts in microbiota was accompanied by a steep reduction in limb regenerative capacity. Fecal microbiota of neotenic and metamorphic Axolotl shared relatively higher similarity, suggesting that diet continues to shape microbiota despite fundamental transformations in the host digestive organs. The results provide novel insights into microbiological and regenerative aspects of Axolotl metamorphosis and will establish a baseline for future in-depth studies.

## Introduction

Metazoan genomes have diversified and evolved in the presence of associated host microbiota. The evolution of morphology and function of animal organ systems may have been influenced by interactions with their microbial partners [1]. From the host perspective, symbioses between metazoans and microbes provide a synergetic impact to operate essential functions for normal growth, development and behavior [2-4]. Studies on host-microbiome interactions in health and disease conditions indicate that perturbation of the crosstalk between the host and microorganisms may lead to deleterious consequences such as developmental defects [3,5] , increased susceptibility to infectious diseases [6,7] and ultimately fitness costs [8]. Even though host genotypes [9] and environmental factors, such as diet and habitat [10,11], were shown to strongly impact the composition and structure of animal microbiota, ecological forces shaping assembly of the host associated microbial communities have still been poorly understood.

Amphibians, which undergo dramatic morphological changes through metamorphosis, exhibit explicitly altered biphasic life stages to tackle developmental challenges. Remarkably, metamorphosis in several marine animal species such as sponges, corals, crabs, sea urchins, an ascidians is mediated by bacterial community [12]. Thyroid hormones (THs) are key players in initiation and completion of metamorphosis [13,14]. Natural accumulation (as in anurans) or administration (as in Axolotl) of THs leads to critical reorganization of organs in order to adapt terrestrial life conditions. This adaptive process includes reconstruction or loss of some existing organs and extremities, and formation of new ones [15,16]. A prominent example of reconstruction is observed in digestive tract of tadpole. In adult frogs acidic stomach and shorter intestine originate from non-acidic

stomach and long intestine of tadpole digestive tract [17,18]. Growing evidence supports the notion that reshaping of organs and composition of microorganisms reciprocally influence each other as functions of bacterial communities are increasingly being linked to host metabolic activities [19-21]. Hence, unraveling microbiome compositions in various life stages may offer new insights into the life stage-specific microbial patterns.

Axolotl (*Ambystoma mexicanum*), a salamander species of amphibians, possess experimentally validated features, such as high regenerative capacity [22], low cancer incidence [23], scarless wound healing [24], life-long neoteny with the ability to undergo induced metamorphosis [25]. These characteristics contributed to the recent establishment of Axolotl as a promising vertebrate model organism for regenerative and developmental biology (reviewed in [26]). Reference resources for this model such as transcriptome [27,28] and a draft genome assembly [29] are publicly available. Current studies on regeneration in Axolotl have focused on identification of genes, gene networks and pathways activated during limb and tail regeneration by utilizing transcriptome and proteome profiling tools [16,27,30,31]. Nevertheless, there is very limited data on microbial diversity of salamanders [32] and systematic investigation of microbiota diversity in multiple organs of salamander species, particularly that of Axolotl, has been missing in the literature.

In this study, we hypothesized that induction of metamorphosis in Axolotl leads to restructuring of bacterial microbiota due to reorganization of tissues via metamorphosis. We then asked whether such microbiota restructuring is accompanied by changes in the host regenerative capacity. To test the hypothesis and answer the question, we explored the variation in neotenic and metamorphic Axolotl's microbiota associated with skin, stomach, gut tissues (crypts), and feces using 16S rRNA gene sequencing and compared

112 limb regenerative capacity between two developmental stages. The results provide novel
113 insights into relationship between perturbed microbial communities due to host factors
114 and putative implication of microbiota in regeneration capacity.
115

116 ## Results

117 Details of the experimental design were described in the methods section (Fig. 1). Within
118 2-3 weeks of hormonal treatment of the animals, we observed weight loss, progressive
119 disappearance of the fin and decrease in the gills size; and in approximately two months
120 all animals showed characteristics of accomplished metamorphosis (Fig. 2a). We first
121 performed comparative analysis of microbiota between neotenic and metamorphic
122 Axolotl organs. We then attempted to answer the question whether shifts in microbiota
123 might be accompanied by a change in host regenerative capacity since previous studies
124 provided evidence that limb regenerative capacity is reduced in metamorphic Axolotl [33].
125 We reproduced these observations in this study that regeneration is indeed impeded in the
126 limbs of metamorphic Axolotl (Fig. 2b). We observed that all neotenic animals (n=15)
127 regenerated (day 64) the limb in a miniaturized form with four digits. In contrast, slower
128 blastema formation and regeneration process were apparent in metamorphic animals. We
129 continued to observe limb generation in metamorphic Axolotls up to day 150. At day 150,
130 2 of 15 metamorphic Axolotls (13 %) restored the limb with four digits. Also, 4 of 15
131 metamorphic animals (27 %) were capable of regenerating amputated limb with 3 digits
132 only. In addition, another 4 animals (27 %) restored limb with only two digits were
133 observed. Rest of the animals (5 out of 15) failed to regenerate a limb to any extent,
134 indicating that the limb generation capacity in metamorphic Axolotls is severely impeded.
135

136 ***Bacterial community structure and membership differ between neotenic and***

***metamorphic Axolotl***

Sequencing of the V3-V4 region of the 16S rRNA gene produced approximately 3.7M reads generated from 27 samples (24 samples from Axolotls and 3 aquarium water samples, hereinafter "Aqua"). The sequences were clustered into 14451 high quality, singleton, chloroplast, and mitochondria removed and chimera-checked Operational Taxonomic Units (OTUs). Average amplicon sequences per sample was 139059 ± 49159 sequences). Our data included 12224 (85% of total) *de novo* OTUs (OTU IDs that begin with "New.Reference" or "New.Cleanup.Reference"). We then classified a representative sequence of these OTUs using RDP classifier (v. 2.2) at 70% bootstrap cutoff. We identified 621 OTUs that did not find hits in the RDP database even at the phylum level ("Unclassified Bacteria"). We thus used MOLE-BLAST to determine their identity. Except a few high abundance OTUs (~5% abundance) enriched in the stomach samples hitting plant mitochondria (discarded), most of these OTUs had abundance below 0.1%, which can be considered a rare OTU [34]. The majority of these OTUs were phylogenetically related to the phylum *Proteobacteria* or *Verrucobacteria* (Supplementary Fig. S1; NCBI Accession numbers: MG518658 - MG519278).

Species richness and diversity were analyzed using a variety of alpha-diversity metrics across neotenic and metamorphic samples (Fig. 3a-d). Metamorphosis significantly reduced diversity in fecal and skin samples as follows; Chao1 and Observed OTUs were significantly lower in fecal and skin samples of the metamorphic samples as compared to neotenic samples (Unpaired Student t test, df=4, $p=0.0018$, $p=0005$, respectively). But Inverse Simpson and Shannon indices were not significantly different ($p=0.34$, $p=0.07$) for these two particular samples although Faith's phylogenetic tree (PD) did indicate that

162 microbiota diversity of these samples were significantly different from each other
163 (*p=0.0022, p=0.0005,* respectively). Both Simpson and Shannon indices take into
164 account richness and evenness in computing the metrics. Therefore, taxa with high
165 relative abundance being heavily weighted in calculations while the indices are less
166 sensitive to rare taxa when compared to richness only metrics [35]. Interestingly, evenness
167 as calculated by Simpson-E index was not significantly different between any sample
168 pairs (*p>0.05* for all comparisons). Correspondingly, we inferred that low abundant taxa
169 drive differences in diversity in fecal and skin samples. Both stomach and gut samples
170 had richness and diversity that were not significantly different on all metrics between
171 neotenic and metamorphic animals (*p>0.05;* Fig. 3a-d).
172
173 Beta diversity of bacterial communities largely differed between neotenic and
174 metamorphic samples based on Bray-Curtis and Jaccard distance metrics (Fig. 4a; and
175 Supplementary Fig. S2, respectively). Within and between group differences (Main-
176 effect) using both distance metric were statistically significant as per PERMANOVA test
177 (*Pseudo-F* (8, 18) = 7.82, *p(Monte Carlo)=0.0001*). Permutational test for homogeneity
178 of dispersions (PERMDISP) was at the border of significance; (F (8, 18) = 8.357, *p*(perm)
179 = 0.0507, 9999 permutations of residuals), indicating that the average within group
180 dispersions were marginally equivalent among groups but dispersion effect, to some
181 degree, may be confounded in the location effect. We next employed Canonical analysis
182 of principal coordinates (CAP, Anderson and Willis, 2003) based on Bray-Curtis distance
183 matrix, a constrained ordination that maximizes the differences among a priori groups and
184 reveals subtle patterns, which otherwise remain elusive to unconstrained ordinations.
185 CAP analysis clearly separated neotenic and metamorphic samples (Fig. 4b) except for
186 the fecal samples (Correct classification rate 96.3%; trace statistics (tr(Q_m'HQ_m):

3,92174 p=0.001 with 9999 permutations, supporting rejection of the null hypothesis of no difference among the sample groups).

*Firmucutes, Proteobacteria,* and *Bacteriodetes* constituted 86.7% ± 8.8 total average abundance across all Axolotl samples (Fig. 5a). Of these phyla, Proteobacteria abundance considerably increased in the skin (5.2% to 41.8%) and in the gut samples (2.7% to 9.1%). In contrast, the abundance of this phylum did not significantly change in the fecal samples yet decreased in the stomach samples (52.0% to 38.9%). Firmicutes abundance seemed to follow the opposite trend. We thus employed Pearson's correlation to identify phylum level taxa (Supplementary Fig. S3) whose abundances negatively correlate as a result of metamorphosis. Abundances of Proteobacteria and Firmicutes along with Verrucomicrobia showed the strongest negative correlation (correlation coefficients were $r$= -0.64 and -0.54, respectively), which was also significant (False Discovery Rate (FDR) adjusted $q$ =0.0027 and 0.026, respectively). Interestingly, the phylum Bacteriodetes abundance in all samples substantially increased after metamorphosis (56.7% vs. 74.2% in fecal samples; 2.5% vs. 29.7% in gut samples; 11.6% vs. 17.5% in skin samples) and negatively correlated with both Firmicutes and Proteobacteria (although this result was not significant ($q$=0.4). Overall, The Axolotl skin microbiota, among others, showed most dramatic shifts between neotenic and metamorphic stages considering these negatively correlated taxa.

Percent average abundances of the genus level taxa are shown in a heatmap (Fig. 5b; for simplicity only taxa abundance ≥ 5% in any sample were shown). Samples were grouped based on Bray-Curtis similarities (top dendogram) and abundances were clustered using hierarchical clustering (average linkage). The observed differences between group

similarities were driven by differences in the relative abundance of multiple bacterial taxa. For example, metamorphic skin samples clustered with stomach samples of neotenic and metamorphic Axolotl; *Clostridium IV*, *Bacteriodes*, and *Sphingomonas* were abundant in these samples. Notably, the genus *Elizabethkingia* were observed in high abundance in the skin and the stomach samples of the metamorphic Axolotl. Metamorphic gut sample clustered with the fecal samples; *Akkermansia and Bacteriodes* being in greater abundance in these samples. Finally, neotenic gut and skin samples were grouped together. This pattern was chiefly due to taxa that could not be classified at genus level (*unclassified Veillonellaceae, unclassified_Ruminococcaceae, unclassified_Lachnospiraceae*) and Clostridium XlVa. Remarkably, Aqua water samples did not have any taxa with high abundance shared with any samples from Axolotl, and separated from other samples.

***Indicator and Shared Species of Neotenic and Metamorphic Axolotl***

We next used DESeq2 analysis, a negative Binomial Wald Test [36,37] to identify differentially abundant taxa ($q<0.01$) in neotenic and metamorphic Axolotl organs at the genus level taxonomy. We also performed indicator species analysis to identify not only abundant and rare OTUs differentially enriched in these samples but also to delineate high fidelity differential patterns (IndVal values $\geq 0.7$, $p<0.01$). We largely observed concordance between both analyses. Skin samples showed the highest number of differentially enriched genera (49 taxa in metamorphic skin samples and 36 taxa enriched in neotenic skin samples); *Pseudonocardia, unclassified_Pseudonocardiaceae, Methylobacterium, Elizabethkingia, Vogesella, Chryseobacterium,* and *Zoogloea* were the top scoring genera in the metamorphic skin while *Limnohabitans* and several taxa that

were classified at higher taxonomic ranking were differentially abundant in the neotenic skin samples (Fig. 6a). These genera were also detected in the indicator species analysis in several OTUs. For example, OTU89, OTU141, OTU1052, OTU1301, OTU1450, OTU2081, were classified as *Pseudonocardia* and OTU89 had the highest abundance of 15.3%. Similarly, the genus *Limnohabitans,* overrepresented in neotenic samples, was assigned to OTU1542 and OTU2587, although both OTUs had relative abundance (0.01%) that can be considered a rare OUT [34]. The following top scoring taxa were differentially abundant in metamorphic and neotenic samples, respectively; Stomach samples: *Elizabethkingia* (OTU335) and *Limnohabitans* (OTU46); gut samples: *Elusimicrobium,* which was not detected by IndVal but OTU7777 (*Hydrogenoanaerobacterium*) was the top scoring taxa (IndVal =0.85, *P* =0.002); *unclassified_Ruminococcaceae, unclassified_Lachnospiraceae* were the indicator species of neotenic gut samples and finally *Odoribacter* (OTU14388), Rikenella (OTU14233) were both differentially abundant and indicator species of metamorphic fecal samples.

Venn diagrams showed number of OTUs shared among or unique for the samples isolated from Axolotl (Supplementary Fig. S4a and Fig. S4b). Number of unique OTUs in all samples of neotenic (7422 OTUs) and metamorphic Axolotl (6237 OTUs) was far grater than shared OTUs indicating assembly of microbiota is tissue specific as in most other animals [38]. In terms of shared OTUs, 368 and 329 OTUs were present in all neotenic and metamorphic samples, respectively. We also collected water samples ("Aqua") from the Aquarium of Axolotl to identify OTUs present in the water that may have colonized the Axolotl skin (Fig. 7a). We found 89 OTUs were shared by the neotenic and metamorphic skin and Aqua samples; 38 OTUs were present only in the neotenic and Aqua samples while 105 OTUs were shared by metamorphic and Aqua samples. However, relative

abundances of all these OTUs were mostly less than 1%. We also compared unique and shared OTUs between gut tissue and fecal samples (Fig. 7b). Exceptionally, the number of OTUs in the metamorphic gut was 4999, representing substantial increase from 2961 OTUs found in the neotenic gut. And the two gut tissue samples shared only 227 OTUs. In stark contrast, the number of unique OTUs decreased to 1365 OTUs whereas neotenic fecal sample had 3408 unique OTUs. Notably, the shared number of fecal and gut OTUs, neotenic or metamorphic, were 288 OTUs and 272 OTUs, suggesting the fecal and gut microbiota are compositionally distinct. Finally, we identified the following genera as core taxa, i.e. shared by 90% of all samples (Core90) (Supplementary Fig. S5): *Bacteroides, Clostridium XlVa, Clostridium XlVb, Akkermansia, Odoribacter, unclassified_Veillonellaceae, unclassified_Lachnospiraceae, Parabacteroides, unclassified_Rhodospirillaceae, unclassified_Ruminococcaceae, Rikenella, unclassified_Clostridiale,* and *Desulfovibrio.*

***Detection of Human taxa in Axolotl Samples and Predicted Functions***

To answer the question if the captive Axolotl may have acquired human bacterial taxa we compared Axolotl microbiota with HMP stool and skin samples (HMP reference data) using weighted and unweighted Unifrac distances (Supplementary Fig. S6 (a-d)). In particular, both neotenic and metamorphic stool and skin samples showed greater similarity to HMP samples compared to other Axolotl samples. These results encouraged us to look at predicted functions of the microbiota using Phylogenetic Investigations of Communities by Reconstruction of Unobserved States (PICRUSt) Due to the specific requirement by PICRUSt, a separate OTU table was generated accordingly using a closed reference analysis based on the GreenGenes 99 database version. CAP analysis of the

287 predicted functions revealed significant differences between the Bray-Curtis distances
288 based on putative pathway abundances (tr(Q_m'HQ_m): 5,78539 p=0.001). However,
289 Bray-Curtis similarities among all distinct groups were around 90%, pointing to the
290 shared predicted functions among the bacterial microbiota of Axolotl organs
291 (Supplementary Fig. S7).
292

293 ## Discussion

294

295 The main purpose of this study was to comparatively characterize bacterial microbiota of
296 Axolotl in neotenic and metamorphic life stages since microbiota of this important
297 biological model has not been reported before. We also asked if differential profiles of
298 Axolotl microbiota in the examined life stages might be accompanied by a change in host
299 regenerative capacity. Our results show that (a)- substantial shifts occurs in the structure
300 and composition of microbiota, particularly in the skin but also in digestive organs; and
301 that (b)- regenerative capacity in the limbs of metamorphic Axolotl steeply diminishes
302 while neotenic Axolotl maintains normal regenerative capacity under identical conditions
303 and that the shifts in the skin microbiota appears to be related to the reduced limb
304 regenerative capacity. Although the scope of this report does not include pinpointing
305 molecular mechanisms accounting for the reduced limb regeneration and its putative
306 association with microbiota, our observations align well with recently published
307 experimental evidence supporting the conclusion that limb regenerative capacity of
308 Axolotl diminishes upon metamorphosis [33,39]. Crucially, our ongoing experiments suggest
309 that reduced regenerative capacity is not observed for some other types of tissues in
310 metamorphic Axolotl (Demircan *et al*., unpublished data).
311

We detected drastic expansion of Proteobacteria in metamorphic Axolotl skin relative to the neotenic skin and noted steep decrease of bacterial diversity in the fecal and skin samples (see Fig. 3). Evidence of skin dysbiosis and the linkage of members of Proteobacteria to reduced regenerative capacity comes from the study by [40]; in this study pathogenic shifts in microbiota and infections were implicated in reduced regeneration in planaria, a model for tissue regeneration; Although the abundance of *Vogesella, Pseudomonas, and Sphingomonas,* all a member of Proteobacteria, and *Chryseobacterium* within Bacteroidetes phylum were virtually not detected in neotenic planarian skin samples, the abundance of these genera considerably increased in the skin of the metamorphic planarian and these genera demonstrably impeded TAK1/MKK/p38 signaling pathway of the innate immunity of the planarian host. Strikingly, our analysis revealed that abundance of these genera and some other members of Proteobacteria known to cause nosocomial infections were, too, highly significantly increased in the metamorphic skin samples from Axolotl (Fig6a and 6b); *Vogesella* ($q$=7.4E-11); *Chryseobacterium* ($q$=5.4E-12); *Undibacterium* ($q$=7.01E-11), and *Sphingomonas* ($q$=4.03E-09). The average abundance of *Pseudomonas*, too, increased (from 0.1% in neotenic skin to 2.2% in metamorphic skin) but the increase was barely significant after FDR correction for multiple testing ($q$=0.056). Furthermore, infiltration of macrophages, as key players of innate immune system, to the site of amputation and cellular signaling pathways in Axolotl were shown to play crucial role in Axolotl limb regeneration [41], lending further credence to the role dysbiotic microbiota can play in reducing the limb regenerative capacity by probably impeding signaling pathways of macrophages. Indeed, macrophages are crucial in removing cellular debris and regulating the balance between fibrosis and scarring [42,43]. Metamorphosis leads to remarkable alterations in immune system such as expression of antimicrobial peptides in epidermis, increase in lymphoid

337 cells ratio and increasingly antigen responsive B cells, and corticosteroid-mediated
338 apoptosis of susceptible lymphocytes [44]. Considering the cross talk between microbes and
339 the immune system, transformation of skin immunity (thickening mucus layer and
340 increased secretion of antimicrobial peptides) may partly account for the disruption of
341 microbiota after metamorphosis. Importantly, disruption in microbiota increases the risk
342 of pathogen infection and overgrowth of opportunistic pathogens during complete
343 metamorphosis as in the example of *Galleria mellonella*, leading to fitness costs [8]. Taken
344 together, the body of evidence on metamorphosing host microbe interactions support the
345 conclusion that dysbiotic restructuring microbiota in Axolotl skin may have contributed
346 to the reduction in limb regeneration. However, further experiments must be performed to
347 ascertain direct mechanistic evidence supporting the cross talk between members of
348 Proteobacteria and blastema pathways involved in regeneration. Future experiments
349 should also include eukaryotic microbiota since fungal skin infections (e.g.
350 chytridiomycosis) in amphibians adversely affects the vital function of amphibian skin
351 [45,46].
352
353 The results from this study add to the emerging appreciation for the broader roles of
354 microbiota in regeneration and wound healing [47-50]. Conceivably, both intrinsic (e.g. age,
355 morphology) and extrinsic factors (e.g. diet, microbiota) may contribute to reduced limb
356 regenerative capacity of the metamorphic Axolotl. Even though we cannot rule out other
357 subtle intrinsic biological factors we selected adult siblings to control for the potentially
358 confounding age factor and to minimize the genetic differences among individuals in this
359 experiment. All animals used in our experiments were also fed on the same diet and
360 maintained under identical conditions. Microbiota is important extrinsic factor profoundly
361 influencing host biology particularly by interacting with the host immune system.

Our results in terms of the composition of Axolotl microbiota broadly parallel the previous reports on microbiota profile of amphibians, and salamanders in particular. Five major dominating phyla, Firmicutes, Bacteroidetes, Proteobacteria, Verrucomicrobia and Actinobacteria were abundant among all studied samples, which is consistent with previous amphibian studies [32,51-54]. Salamander microbiota was previously studied but often distinct species of salamander skin microbiota was profiled [51,53] and systematic investigation of microbiota diversity in multiple organs of salamander species, particularly that of Axolotl, has been missing in the literature with few exception. Bletz *et al.* (2016) characterized both gut and skin microbiota of fire salamanders within the natural habitat. Surprisingly, like captive Axolotl in this study, the wild salamanders' gut and skin are associated with the above mentioned five major phyla. The genera *Chryseobacterium*, *Pseudomonas, Flavobacterium, Sphingobacterium, Novosphingobium,* were reported to be dominant taxa in skin of fire salamander living in nature. Interestingly, we detected these genera in the neotenic skin samples in this study albeit in low abundance but substantially increased in abundance in the metamorphic skin. These bacterial genera belong to a large, ecologically diverse group, and their members include known pathogens; some could be opportunistic while some others can outcompete emerging fungal pathogens [55]. Interestingly, our analysis revealed that metamorphic Axolotl skin was dominated by *Pseudonocardia* (15.7% ± 10.4), and an unclassified taxa from *Pseudonocardiaceae* family (9.7% ± 5.7), both are indicator species of the metamorphic skin (IndVal =0.99, $p$=0.006). *Pseudonocardia spp*. is a well known antifungal commensal microorganism [56] and colonize on the integument of fungus-gardening ant species. Recruitment of the members of this genus in high abundance by metamorphic Axolotl might reflect host-symobiont synergy against

387 pathogenic fungi.

388

389 We sequenced pools of water samples from the Axolotl aquarium ("Aqua") to identify
390 water-borne bacterial taxa acquired by Axolotls. Surprisingly, most abundant genera of
391 Aqua samples (e.g. *Acidovorax, Armatimonas, Flectobacillus*) were not associated with
392 Axolotl organs but only a subset of low-abundance bacteria was detected. For example,
393 *Aquabacterium* abundance in metamorphic skin and neotenic stomach were 3.9% and
394 7.3%, respectively while its abundance in Aqua sample was 0.1%. Our results are
395 consistent with previous work reporting amphibian skin may select rare taxa from the
396 environment [51-53,57,58]. In this study, we found that 89 out of 509 OTUs in Aqua samples
397 were present in neotenic skin samples while 105 OTUs shared between Aqua and
398 metamorphic skin samples (see Fig. 6), and 150 shared OTUs with Aqua samples, the
399 highest among others, with metamorphic stomach samples. Consequently, our results
400 support the notion that both host and external factors shape the host microbiota but host
401 genetics applies selective filter.

402

403 Conversely, diet is another crucial factor strongly influencing structure of gut microbiota
404 of animal host and even dominate host genotype [59]. Although host genotype and diet are
405 constant in this study, metamorphosis is likely to cause remodeling of epigenetic
406 landscape in the host genome, which in turn is expected to reshape microbiota. Notably,
407 fecal samples from the neotenic and metamorphic Axolotls clustered together, albeit
408 richness in metamorphic fecal samples significantly decreased. We observed that feeding
409 behavior of the metamorphic Axolotl change during metamorphosis, the animals tend to
410 eat less often (low appetite), which might account for the decreased fecal diversity.
411 Although no major restructuring of intestine *via* metamorphosis was apparent as

412 described before [16], we observed a higher number of goblet cells and thicker mucus layer
413 in the metamorphic gut tissue compared to neotenic gut (Supplementary Fig. S8). Taken
414 together, relative influence of diet and host epigenetics seems to be compartmentalized;
415 diet appears to influence strongly the bacterial diversity in the fecal microbiota in the gut
416 lumen whereas the host epigenetics (and the resulting changes in transcriptome due to
417 metamorphosis) seems to play a greater and selective role in gut tissues (crypts). Some
418 genera, often associated with symbiosis such as *Alistipes* and *Elusimicrobium*, were
419 differentially enriched in the metamorphic gut tissues whereas neotenic gut tissues were
420 represented by two genera with *unclassified Clostridiaceae* and *unclassified*
421 *Enterobacteriaceae*. Suprisingly, the abundance of *Akkermansia* considerably increased
422 in the metamorphic gut tissues (16%) relative to neotenic gut (9%). *A. muciniphila* within
423 this genus is known to be a mucin degrading and symbiotic bacterium and the increase in
424 abundance of this genus is meaningful with increasingly thicker mucus layer we observed
425 in the metamorphic gut tissue staining.
426
427 Our analysis revealed that Axolotl microbiota to certain extent was "humanized" in
428 captivity as manifested from similarity of gut and skin microbiota with the human
429 microbiota, which prompted us to compare predicted functions using PICRUSt [60], which
430 is optimized for human microbiota. We found that all samples included in microbiota
431 analysis were highly similar based on the abundance of predicted microbial genes (40%).
432 Though further study using shotgun metagenomics technology is warranted, our findings
433 raise the possibility that deficiency in the microbial community function in a given organ
434 can be possibly compensated without taxonomic coherence. However, caution should be
435 exercised in interpreting these results considering the accuracy of the predicted functions
436 is predicated on the closed reference database, whereas the majority of OTUs in this study

were clustered using open reference.

## Conclusions

Our study shows microbiota inhabiting Axolotl organs considerably restructure upon metamorphosis and expansion of opportunistic bacteria within Proteobacteria may be contributing to the reduced limb regenerative capacity. These results must be taken into consideration when captive Axolotl is employed in regeneration studies. Lack of systematic studies on Axolotl microbiota has hindered its potential as a fruitful model in host-microbe interaction studies. Therefore, the data presented here make a significant contribution for further characterization of a valuable biological model for regeneration, aging, and stem cell research.

## Methods

### Ethical statement and experimental design

The local ethics committee of the Istanbul Medipol University (IMU) authorized experimental protocols and animal care conditions (the authorization number: 38828770-E.7856). All experiments were performed in accordance with relevant guidelines and regulations. The experimental design followed in this study is depicted in Fig. 1. Briefly, a total of 48 adult Axolotls (12-15 cm in length, 1 year old) were obtained from the animal care facility of the IMU. Axolotls were chosen from among the siblings. Out of 48 Axolotls 30 were reserved for amputation/limb regeneration experiments; and 18 out of 48 were used for metamorphosis experiments; half of both groups (15 for regeneration experiments and 9 for metamorphosis; 24 total) were then induced individually to undergo metamorphosis by L-thyroxine (Sigma-Aldrich, St Louis, MO, USA, Cat. No.

462 T2376) as described elsewhere [25]. Briefly, T4 solution was prepared by dissolving L-
463 thyroxine in Holtfreter's solution (final concentration 50 nM) and was administrated to
464 animals that were maintained individually throughout the experimental period. The
465 medium was replaced with freshly prepared T4 containing solution every third day and
466 animals were monitored for morphological changes. Administration of the hormone
467 continued for another 3 weeks until fully metamorphic Axolotls were obtained. Both
468 neotenic and metamorphic animals were maintained in individual aquaria water at 18 ± 2
469 °C in Holtfreter's solution. Axolotls were maintained in the university animal facility
470 within a batch-flow aquarium system where the batch water was treated with UV light
471 and filtered to prevent infections. All animals were kept in the same aquatic solution and
472 fed with same diet. Animals were fed once a day using a staple food (JBL Novo LotlM,
473 Neuhofen, Germany). Axolotls did not receive any antibiotic treatment throughout the
474 experiments.

475

476 **Sample collection**

477

478 Animals were sacrificed using 0.2% MS222 (Sigma-Aldrich, St Louis, MO, USA. Cat.
479 No. E10521) approximately in two months upon visual observation of metamorphosis.
480 Neotenic and metamorphic animals formed two major experimental groups. Randomly
481 selected three animals were grouped to have three replicates (R1, R2 and R3) for neotenic
482 and metamorphic experimental groups (Fig. 1). For each replicate skin, stomach, intestine
483 and fecal samples were harvested from three animals and pooled together under sterile
484 conditions in a bio safety cabin. To collect the skin samples, animals were rinsed in sterile
485 water to get rid of the transient bacteria. As the next step, skin samples from the mid
486 stylopod level of the right forelimb were isolated for each replicates with punch biopsy

using disposable and sterile 6 mm diameter punches (Miltex, York, PA, USA). Stomach and intestine samples were collected after dissection of animals. Intestine contents were first removed, split into approximately equal 4-5 pieces, and rinsed with sterile serum physiologic solution five times. Fecal samples were harvested from the rectum. Isolated and pooled samples for each replicate were frozen in liquid nitrogen immediately for cryopreservation. All samples were stored at −80°C till DNA isolation. To compare harvested samples with the microbial structure of Holtfreter's solution ("Aqua" samples), water samples from randomly chosen aquariums (n=9) were collected and 3 samples were pooled together to have three replicates (R1, R2 and R3).

**Amputation**

A total of 30 Axolot were used for regeneration experiments. Half of the animals were induced to undergo metamorphosis by T4 administration as described above. After complete metamorphosis was achieved, right forelimb of both neotenic and metamorphic animals were amputated from the mid-stylopod site Both macroscopic and microscopic pictures were taken by using Nikon D3200 camera and Zeiss Axio zoom V16 microscope, respectively. Animals were anesthetized in 0.1% MS222 (Sigma-Aldrich, St Louis, MO, USA. Cat. No. E10521) for all animal procedures.

**Histology**

Removal of fecal from the isolated intestine samples was followed by fixation in 10% neutral buffered formalin (NBF) for 48 h. The samples were then processed by immersion of materials in ascending alcohol series, toluene and embedding in paraffin. 4 μm thick tissue sections were obtained by using microtome. Sections were deparaffinized and

512 stained with Hematoxylin and Eosin (Bio-Optica Mayer's Hematoxylin and Eosin Y
513 Plus), Masson's Trichrome (KIT, Masson Trichrome with aniline blue, Bio Optica, 04-
514 010802), Alcian Blue (KIT, Alcian Blue Acid Mucopolusaccharides staining, Bio-Optica,
515 04-160802) according to manufacturer's instructions. Images were taken by using the
516 NIKON DS-Fi2-U3 Digital Camera. The detailed protocol was described in a previous
517 work [16].
518
519 **DNA extraction**
520
521 DNA isolation from the skin, intestine, and stomach samples was carried out with
522 DNeasy Blood & Tissue kit (Qiagen) according to the manufacturer's protocol. QIAamp
523 DNA Stool Mini Kit (Qiagen) was used to extract the DNA of the fecal samples by
524 following the manufacturer's recommendations. To extract DNA from the water samples
525 were first filtered through filters with 0.2 μm pore size and the filter papers subsequently
526 were used in DNA extractions using metagenomic DNA Isolation Kit for Water
527 (Epicentre, Cat. No. MGD08420) by following the producer's protocol. Spectramax i3
528 (Molecular Devices, Sunnyvale, CA) was used to measure the concentrations of isolated
529 DNA. Quality of DNA samples was checked by electrophoresis in 1.0% agarose gels.
530
531 **PCR and sequencing of 16S rRNA amplicons**
532
533 To amplify the variable V3-V4 regions of the 16S rRNA gene, the primers 341F (5′-
534 CCTACGGGNGGCWGCAG -3′) and 805R (5′- GACTACHVGGGTATCTAATCC-3′)
535 were used [61]. MiSeq sequencing adaptor sequences were added to the 5′ ends of forward
536 and reverse primers. Approximately 12.5 ng of purified DNA from each sample was used

as a template for PCR amplification in 25 µl reaction mixture by using 2x KAPA HiFi HotStart ReadyMix (Kapa Biosystems, MA, USA). For PCR amplification, the following conditions were followed: denaturation at 95°C for 3 min., followed by 25 cycles of denaturation at 95°C for 30 sec., annealing at 55°C for 30 sec. and extension at 72°C for 30 sec., with a final extension at 72°C for 5 min. No template negative control samples were included to check PCR contamination and none of the negative controls yielded detectable level of amplification on agarose gels. Amplified PCR products were purified with Agencourt AMPure XP purification system (Beckman Coulter) and Nextera PCR was performed by using sample-specific barcodes. Constructed Nextera library was then sequenced by Illumina MiSeq platform using MiSeq Reagent Kit v3.

**Sequence processing, clustering, and taxonomic assignment**

To analyze the paired-end sequencing data Quantitative Insights Into Microbial Ecology (QIIME, v1.9.1) [62] software was used at the Nephele platform (v.1.6, 2016) of the National Institute of Allergy and Infectious Diseases (NIAID, Bethesda, MD). Nephele platform was also used for the Phylogenetic investigation of communities by reconstruction of unobserved states (PICRUSt) analysis [60] and for comparing the data with the Human Microbiome Project (HMP). Before submitting the raw reads into the Nephele pipeline, primers were removed using cutadapt program [63] and the pipeline was stringently configured to perform the following steps; reads below average quality scores ($q<30$) and read-length >450 bp were eliminated. After joining the pair-end reads, the reads were clustered into operational taxonomic units (OTUs) using open reference OTU-picking strategy [64]. The open-reference approach initially runs a closed-reference step. Sequences that fail closed-reference assignment are then clustered as *de novo* OTU based

562 on pairwise similarity among all sequences in the data set. Open reference clustering was
563 performed based on the 97% clustered SILVA reference (SILVA 123 release; ) database
564 [65] and SortMeRNA combined with SUMACLUST algorithms [66]. Non-matching reads to
565 closed reference were subsequently clustered *de novo.* After obtaining the OTU table
566 from the pipeline, UCHIME (v.4.2) program (http://drive5.com/uchime) integrated into
567 the Mothur (v.1.39.5) tool [67] was separately run to remove chimeric reads. Additionally,
568 The RDP classifier [68] (v. 2.2) was locally run to assign taxonomy for each OTU at a
569 confidence greater than 70% cutoff. Reads that could not be classified at the genus level
570 were sequentially assigned to higher taxonomic hierarchy up to the kingdom level.
571 Unclassified reads at the kingdom level ("Unclassified Bacteria") were extracted from the
572 OTU-representative sequences and searched for nearest neighbor method using MOLE-
573 BLAST [69]. This tool computes a multiple sequence alignment (MSA) between the query
574 sequences along with their top BLAST database hits, and generates a phylogenetic tree.
575 Species richness and diversity were estimated by QIIME with the following alpha
576 diversity metrics: OTU richness, Chao1, Shannon, Simpson E, Inverse Simpson, and
577 Faith's phylogenetic diversity (PD). We assessed normality of alpha diversity data using
578 Shapiro-Wilk tests and compared the metrics between neotenic and metamorphic
579 microbiota using unpaired two-tailed *t*-test. Venn diagrams were constructed using jvenn,
580 a web based tool (http://jvenn.toulouse.inra.fr) [70].
581
582 **Multivariate analysis of community structures and diversity**
583
584 Bray–Curtis similarity index [71] and Jaccard index of similarity [72] were used to obtain
585 distance matrix after standardizing by the column sums and transforming (square-root)
586 the read abundance data. Similarities in microbial community structures among samples

were first displayed using principal coordinate analysis (PCO) (unconstrained). Differences in community structure related to metamorphosis were displayed using a constrained ordination technique, Canonical Analysis of Principal coordinates (CAP). Tests of the multivariate null hypotheses of no differences among a priori defined groups were examined using PERMANOVA and the CAP classification success rate. CAP uses PCO followed by canonical discriminant analysis to provide a constrained ordination that maximizes the differences among a priori groups and reveals patterns that cannot be unraveled using unconstrained ordinations [73]. CAP classification success rates and CAP $trace_{Q\_m0HQ\_m}$ statistics were examined in combination to draw conclusions about separation of a priori groups. Permutational analysis of multivariate dispersions (PERMDISP) [74] was used to test for heterogeneity of community structure in a priori groups. PERMANOVA, CAP and PERMDISP were performed with 9999 permutations and run as routines in PRIMER6 [75].

To delineate bacterial taxa responsible for the multivariate patterns and differentially enriched taxa between the neotenic and metamorphic Axolotl organs, we used DESeq2, a negative Binomial Wald Test [36,37] and indicator species analysis [76]. DESeq2 analysis results, along with core OTU heatmap, phylum correlation heatmap, and read count figures were obtained using MicrobiomeAnalyst [77]. To perform indicator species analysis, R package labdsv was used. Boxplots, barchart, bubbleplots, and heatmaps were generated using R packages including vegan, ggplot2, heatmap2, Heatplus, reshape, colorramps, and RcolorBrewer (R Core Team 2016, http://www.r-project.org).

**Availability of data and materials**

The datasets generated and/or analysed during the current study are available in the figshare repository: https://figshare.com/s/b1f232d8d054e0e20f06

## References


1 McFall-Ngai, M. *et al.* Animals in a bacterial world, a new imperative for the life sciences. *Proc Natl Acad Sci U S A* **110**, 3229-3236, doi:10.1073/pnas.1218525110 (2013).

2 Diaz Heijtz, R. *et al.* Normal gut microbiota modulates brain development and behavior. *Proc Natl Acad Sci U S A* **108**, 3047-3052, doi:10.1073/pnas.1010529108 (2011).

3 Hsiao, E. Y. *et al.* Microbiota modulate behavioral and physiological abnormalities associated with neurodevelopmental disorders. *Cell* **155**, 1451-1463, doi:10.1016/j.cell.2013.11.024 (2013).

4 Sommer, F. & Backhed, F. The gut microbiota--masters of host development and physiology. *Nat Rev Microbiol* **11**, 227-238, doi:10.1038/nrmicro2974 (2013).

5 Kostic, A. D., Howitt, M. R. & Garrett, W. S. Exploring host-microbiota interactions in animal models and humans. *Genes Dev* **27**, 701-718, doi:10.1101/gad.212522.112 (2013).

6 Baumler, A. J. & Sperandio, V. Interactions between the microbiota and pathogenic bacteria in the gut. *Nature* **535**, 85-93, doi:10.1038/nature18849 (2016).

7 Sekirov, I. *et al.* Antibiotic-induced perturbations of the intestinal microbiota alter host susceptibility to enteric infection. *Infect Immun* **76**, 4726-4736, doi:10.1128/IAI.00319-08 (2008).

8 Johnston, P. R. & Rolff, J. Host and Symbiont Jointly Control Gut Microbiota during Complete Metamorphosis. *PLOS Pathogens* **11**, e1005246, doi:10.1371/journal.ppat.1005246 (2015).

9 Spor, A., Koren, O. & Ley, R. Unravelling the effects of the environment and host genotype on the gut microbiome. *Nat Rev Micro* **9**, 279-290, doi:http://www.nature.com/nrmicro/journal/v9/n4/suppinfo/nrmicro2540_S1.html (2011).

10 Amato, K. R. *et al.* Habitat degradation impacts black howler monkey (Alouatta pigra) gastrointestinal microbiomes. *ISME J* **7**, 1344-1353, doi:10.1038/ismej.2013.16 (2013).

11 Bletz, M. C. *et al.* Host Ecology Rather Than Host Phylogeny Drives Amphibian Skin Microbial Community Structure in the Biodiversity Hotspot of Madagascar. *Frontiers in Microbiology* **8**, 1530, doi:10.3389/fmicb.2017.01530 (2017).

12 Shikuma, N. J., Antoshechkin, I., Medeiros, J. M., Pilhofer, M. & Newman, D. K. Stepwise metamorphosis of the tubeworm Hydroides elegans is mediated by a bacterial inducer and MAPK signaling. *Proc Natl Acad Sci U S A* **113**, 10097-10102 (2016).

13 Kikuyama, S., Kawamura, K., Tanaka, S. & Yamamoto, K. Aspects of amphibian metamorphosis: hormonal control. *Int Rev Cytol* **145**, 105-148 (1993).

14 Tata, J. R. Amphibian metamorphosis as a model for the developmental actions of thyroid hormone. *Molecular and Cellular Endocrinology* **246**, 10-20, doi:https://doi.org/10.1016/j.mce.2005.11.024 (2006).

15 Brown, D. D. & Cai, L. Amphibian metamorphosis. *Dev Biol* **306**, 20-33, doi:10.1016/j.ydbio.2007.03.021 (2007).

16 Demircan, T. *et al.* A histological atlas of the tissues and organs of neotenic and metamorphosed axolotl. *Acta Histochemica* **118**, 746-759, doi:https://doi.org/10.1016/j.acthis.2016.07.006 (2016).

17 Hourdry, J., L'Hermite, A. & Ferrand, R. Changes in the Digestive Tract and Feeding Behavior of Anuran Amphibians during Metamorphosis. *Physiological Zoology* **69**, 219-251 (1996).

18 Stevens, C. E. & Hume, I. D. *Comparative physiology of the vertebrate digestive system*. (Cambridge University Press
, 2004).

19 Boulange, C. L., Neves, A. L., Chilloux, J., Nicholson, J. K. & Dumas, M. E. Impact of the gut microbiota on inflammation, obesity, and metabolic disease. *Genome Med* **8**, 42, doi:10.1186/s13073-016-0303-2 (2016).

20 den Besten, G. *et al.* The role of short-chain fatty acids in the interplay between diet, gut microbiota, and host energy metabolism. *J. Lipid Res.* **54**, 2325-2340, doi:10.1194/jlr.R036012 (2013).

21 Musso, G., Gambino, R. & Cassader, M. Interactions Between Gut Microbiota and Host Metabolism Predisposing to Obesity and Diabetes. *Annual Review of Medicine* **62**, 361-380, doi:10.1146/annurev-med-012510-175505 (2011).

22 Roy, S. & Gatien, S. Regeneration in axolotls: a model to aim for! *Experimental Gerontology* **43**, 968-973, doi:https://doi.org/10.1016/j.exger.2008.09.003 (2008).

23 Oviedo, N. J. & Beane, W. S. Regeneration: The origin of cancer or a possible cure? *Semin Cell Dev Biol* **20**, 557-564, doi:10.1016/j.semcdb.2009.04.005 (2009).

24 Denis, J.-F., Lévesque, M., Tran, S. D., Camarda, A.-J. & Roy, S. Axolotl as a Model to Study Scarless Wound Healing in Vertebrates: Role of the Transforming Growth Factor Beta Signaling Pathway. *Advances in Wound Care* **2**, 250-260, doi:10.1089/wound.2012.0371 (2013).

25 Page, R. B. & Voss, S. R. Induction of metamorphosis in axolotls (Ambystoma mexicanum). *Cold Spring Harb Protoc* **2009**, pdb prot5268, doi:10.1101/pdb.prot5268 (2009).

26 Voss, S. R., Epperlein, H. H. & Tanaka, E. M. Ambystoma mexicanum, the axolotl: a versatile amphibian model for regeneration, development, and evolution studies. *Cold Spring Harb Protoc* **2009**, pdb emo128, doi:10.1101/pdb.emo128 (2009).

27 Bryant, D. M. *et al.* A tissue-mapped axolotl de novo transcriptome enables identification of limb regeneration factors. *Cell reports* **18**, 762-776, doi:10.1016/j.celrep.2016.12.063 (2017).

28 Jiang, P. *et al.* Analysis of embryonic development in the unsequenced axolotl: Waves of transcriptomic upheaval and stability. *Dev Biol* **426**, 143-154, doi:10.1016/j.ydbio.2016.05.024 (2017).

29 Keinath, M. C. *et al.* Initial characterization of the large genome of the salamander Ambystoma mexicanum using shotgun and laser capture chromosome sequencing. *Scientific Reports* **5**, 16413, doi:10.1038/srep16413 https://www.nature.com/articles/srep16413 - supplementary-information (2015).

30 King, B. L. & Yin, V. P. A Conserved MicroRNA Regulatory Circuit Is Differentially Controlled during Limb/Appendage Regeneration. *PLOS ONE* **11**, e0157106, doi:10.1371/journal.pone.0157106 (2016).

31 Wu, H. J. & Wu, E. The role of gut microbiota in immune homeostasis and autoimmunity. *Gut Microbes* **3**, 4-14, doi:10.4161/gmic.19320 (2012).

32 McKenzie, V. J., Bowers, R. M., Fierer, N., Knight, R. & Lauber, C. L. Co-habiting amphibian species harbor unique skin bacterial communities in wild populations. *ISME J* **6**, 588-596, doi:10.1038/ismej.2011.129 (2012).

33 Monaghan, J. R. *et al.* Experimentally induced metamorphosis in axolotls reduces regenerative rate and fidelity. *Regeneration* **1**, 2-14, doi:10.1002/reg2.8 (2014).

34 Lynch, M. D. J. & Neufeld, J. D. Ecology and exploration of the rare biosphere. *Nat Rev Micro* **13**, 217-229, doi:10.1038/nrmicro3400 (2015).

35 Bent, S. J. & Forney, L. J. The tragedy of the uncommon: understanding limitations in the analysis of microbial diversity. *ISME J* **2**, 689-695, doi:10.1038/ismej.2008.44 (2008).

36 Love, M. I., Huber, W. & Anders, S. Moderated estimation of fold change and dispersion for RNA-seq data with DESeq2. *Genome Biol* **15**, 550, doi:10.1186/s13059-014-0550-8 (2014).

37 McMurdie, P. J. & Holmes, S. Waste Not, Want Not: Why Rarefying Microbiome Data Is Inadmissible. *PLOS Computational Biology* **10**, e1003531, doi:10.1371/journal.pcbi.1003531 (2014).

38 Donaldson, G. P., Lee, S. M. & Mazmanian, S. K. Gut biogeography of the bacterial microbiota. *Nature reviews. Microbiology* **14**, 20-32, doi:10.1038/nrmicro3552 (2016).

39 Seifert, A. W., Monaghan, J. R., Voss, S. R. & Maden, M. Skin Regeneration in Adult Axolotls: A Blueprint for Scar-Free Healing in Vertebrates. *PLoS ONE* **7**, e32875, doi:10.1371/journal.pone.0032875 (2012).

40 Arnold, C. P. *et al.* Pathogenic shifts in endogenous microbiota impede tissue regeneration via distinct activation of TAK1/MKK/p38. *Elife* **5**, doi:10.7554/eLife.16793 (2016).

41 Godwin, J. W., Pinto, A. R. & Rosenthal, N. A. Macrophages are required for adult salamander limb regeneration. *Proceedings of the National Academy of Sciences of the United States of America* **110**, 9415-9420, doi:10.1073/pnas.1300290110 (2013).

42 Mescher, A. L. Macrophages and fibroblasts during inflammation and tissue repair in models of organ regeneration. *Regeneration* **4**, 39-53, doi:10.1002/reg2.77 (2017).

43 Stramer, B. M., Mori, R. & Martin, P. The inflammation-fibrosis link? A Jekyll and Hyde role for blood cells during wound repair. *J Invest Dermatol* **127**, 1009-1017, doi:10.1038/sj.jid.5700811 (2007).

44 Ussing, A. P. & Rosenkilde, P. Effect of Induced Metamorphosis on the Immune System of the Axolotl, Ambystoma mexicanum. *General and Comparative Endocrinology* **97**, 308-319, doi:https://doi.org/10.1006/gcen.1995.1031 (1995).

45 Bales, E. K. *et al.* Pathogenic Chytrid Fungus Batrachochytrium dendrobatidis, but Not B. salamandrivorans, Detected on Eastern Hellbenders. *PLOS ONE* **10**, e0116405, doi:10.1371/journal.pone.0116405 (2015).

46 Martel, A. *et al.* Batrachochytrium salamandrivorans sp. nov. causes lethal chytridiomycosis in amphibians. *Proceedings of the National Academy of Sciences of the United States of America* **110**, 15325-15329, doi:10.1073/pnas.1307356110 (2013).

47 Gardiner, M. *et al.* A longitudinal study of the diabetic skin and wound microbiome. *PeerJ* **5**, e3543, doi:10.7717/peerj.3543 (2017).

48 Grice, E. A. *et al.* Longitudinal shift in diabetic wound microbiota correlates with prolonged skin defense response. *Proc Natl Acad Sci U S A* **107**, 14799-14804, doi:10.1073/pnas.1004204107 (2010).

49 Naito, T. *et al.* Lipopolysaccharide from Crypt-Specific Core Microbiota Modulates the Colonic Epithelial Proliferation-to-Differentiation Balance. *MBio* **8**, doi:10.1128/mBio.01680-17 (2017).

50 Wu, X. *et al.* Oral ampicillin inhibits liver regeneration by breaking hepatic innate immune tolerance normally maintained by gut commensal bacteria. *Hepatology* **62**, 253-264, doi:10.1002/hep.27791 (2015).

51 Bletz, M. C. *et al.* Amphibian gut microbiota shifts differentially in community structure but converges on habitat-specific predicted functions. *Nat Commun* **7**, 13699, doi:10.1038/ncomms13699 (2016).

52 Bletz, M. C., Perl, R. G. B. & Vences, M. Skin microbiota differs drastically between co-occurring frogs and newts. *Royal Society Open Science* **4**, 170107, doi:10.1098/rsos.170107 (2017).

53 Sanchez, E. *et al.* Cutaneous Bacterial Communities of a Poisonous Salamander: a Perspective from Life Stages, Body Parts and Environmental Conditions. *Microb Ecol* **73**, 455-465, doi:10.1007/s00248-016-0863-0 (2017).

54 Weng, F. C., Yang, Y. J. & Wang, D. Functional analysis for gut microbes of the brown tree frog (Polypedates megacephalus) in artificial hibernation. *BMC Genomics* **17**, 1024, doi:10.1186/s12864-016-3318-6 (2016).

55 Lauer, A., Simon, M. A., Banning, J. L., Lam, B. A. & Harris, R. N. Diversity of cutaneous bacteria with antifungal activity isolated from female four-toed salamanders. *ISME J* **2**, 145-157, doi:10.1038/ismej.2007.110 (2008).

56 Sen, R. *et al.* Generalized antifungal activity and 454-screening of Pseudonocardia and Amycolatopsis bacteria in nests of fungus-growing ants. *Proc Natl Acad Sci U S A* **106**, 17805-17810, doi:10.1073/pnas.0904827106 (2009).

57 Kueneman, J. G. *et al.* The amphibian skin-associated microbiome across species, space and life history stages. *Mol Ecol* **23**, 1238-1250, doi:10.1111/mec.12510 (2014).

58 Walke, J. B. *et al.* Amphibian skin may select for rare environmental microbes. *ISME J* **8**, 2207-2217, doi:10.1038/ismej.2014.77 (2014).

59 Carmody, R. N. *et al.* Diet dominates host genotype in shaping the murine gut microbiota. *Cell Host Microbe* **17**, 72-84, doi:10.1016/j.chom.2014.11.010 (2015).

60 Langille, M. G. I. *et al.* Predictive functional profiling of microbial communities using 16S rRNA marker gene sequences. *Nature biotechnology* **31**, 814-821, doi:10.1038/nbt.2676 (2013).

61 Walters, W. *et al.* Improved Bacterial 16S rRNA Gene (V4 and V4-5) and Fungal Internal Transcribed Spacer Marker Gene Primers for Microbial Community Surveys. *mSystems* **1**, doi:10.1128/mSystems.00009-15 (2016).

62 Caporaso, J. G. *et al.* QIIME allows analysis of high-throughput community sequencing data. *Nat Methods* **7**, 335-336, doi:10.1038/nmeth.f.303 (2010).

63 Martin, M. Cutadapt removes adapter sequences from high-throughput sequencing reads. *EMBnet.journal* **17**, 10-12 (2011).

64 Rideout, J. R. *et al.* Subsampled open-reference clustering creates consistent, comprehensive OTU definitions and scales to billions of sequences. *PeerJ* **2**, e545, doi:10.7717/peerj.545 (2014).

65 Quast, C. *et al.* The SILVA ribosomal RNA gene database project: improved data processing and web-based tools. *Nucleic Acids Res* **41**, D590-596, doi:10.1093/nar/gks1219 (2013).

66 Kopylova, E. *et al.* Open-Source Sequence Clustering Methods Improve the State Of the Art. *mSystems* **1**, doi:10.1128/mSystems.00003-15 (2016).

67 Schloss, P. D. *et al.* Introducing mothur: Open-Source, Platform-Independent, Community-Supported Software for Describing and Comparing Microbial Communities. *Applied and Environmental Microbiology* **75**, 7537-7541, doi:10.1128/AEM.01541-09 (2009).

68 Wang, Q., Garrity, G. M., Tiedje, J. M. & Cole, J. R. Naïve Bayesian Classifier for Rapid Assignment of rRNA Sequences into the New Bacterial Taxonomy. *Applied and Environmental Microbiology* **73**, 5261-5267, doi:10.1128/AEM.00062-07 (2007).

69 Ncbi Resource Coordinators. Database resources of the National Center for Biotechnology Information. *Nucleic Acids Research* **43**, D6-D17, doi:10.1093/nar/gku1130 (2015).

70 Bardou, P., Mariette, J., Escudié, F., Djemiel, C. & Klopp, C. jvenn: an interactive Venn diagram viewer. *BMC Bioinformatics* **15**, 293, doi:10.1186/1471-2105-15-293 (2014).

71 Bray, J. R. & Curtis, J. T. An Ordination of the Upland Forest Communities of Southern Wisconsin. *Ecological Monographs* **27**, 325-349, doi:10.2307/1942268 (1957).

72 Jaccard, P. Nouvelles recherches sur la distribution florale. *Bull. Soc. Vaudoise Sci. Nat.* **44**, 223-270 (1908).

73 Anderson, M. J. & Willis, T. J. CANONICAL ANALYSIS OF PRINCIPAL COORDINATES: A USEFUL METHOD OF CONSTRAINED ORDINATION FOR ECOLOGY. *Ecology* **84**, 511-525, doi:10.1890/0012-9658(2003)084[0511:CAOPCA]2.0.CO;2 (2003).

74 Anderson, M. J. Distance-based tests for homogeneity of multivariate dispersions. *Biometrics* **62**, 245-253, doi:10.1111/j.1541-0420.2005.00440.x (2006).

75 Clarke, K. & Gorley, R. N. *Primer v6:User Manual/Tutorial*. (PRIMER-E, 2006).

76 Dufrêne, M. & Legendre, P. SPECIES ASSEMBLAGES AND INDICATOR SPECIES:THE NEED FOR A FLEXIBLE ASYMMETRICAL APPROACH. *Ecological Monographs* **67**, 345-366, doi:10.1890/0012-9615(1997)067[0345:SAAIST]2.0.CO;2 (1997).

77 Dhariwal, A. *et al.* MicrobiomeAnalyst: a web-based tool for comprehensive statistical, visual and meta-analysis of microbiome data. *Nucleic Acids Research* **45**, W180-W188, doi:10.1093/nar/gkx295 (2017).

## Acknowledgements

This study was financially supported by the Medipol University Research Fund. This study used the Nephele platform from the National Institute of Allergy and Infectious Diseases (NIAID) Office of Cyber Infrastructure and Computational Biology (OCICB) in Bethesda, MD.

## Author contributions statement

TD and SY conceived the study. TD, BY, İK, AEİ and ECF performed animal experiments. TD, GÖ, and SY acquired sequencing data; TD, GO, and SY analyzed and interpreted the data. TD, GO, GÖ, and SY drafted and critically reviewed/revised the manuscript. All authors read and approved the final manuscript.

## Additional Information

## Competing interests

The authors of this manuscript declare no competing interests.

## FIGURE LEGENDS

**Figure 1. Experimental design for the comparison of neotenic and metamorphic Axolotl**. Of 48 siblings, a subset of 24 animals (9 animals for metamorphosis and 15

874 animals for regeneration experiments) were randomly selected and induced
875 metamorphosis by T4 hormone administration while the rest kept untreated in neoteny. 30
876 animals (15 neotenic and 15 metamorphosed) were used in regeneration experiments and
877 18 animals (9 neotenic and 9 metamorphic) were housed for microbiome analysis. Each
878 sample groups for skin, gut, stomach and fecal samples consisted of 3 replicates
879 following randomization and pooling.
880
881 **Figure 2. Time course of metamorphosis and limb regeneration.** Time course (Day0 -
882 Day72) after T4 administration showing anatomical changes to adapt terrestrial life
883 conditions. Metamorphosis-associated characteristics such as weight loss and
884 disappearance of fin and gills were noticed gradually within this time period. **(a).** Time
885 course (Day0 - Day64) after limb amputation demonstrating differences between
886 regenerative capacity of neotenic (upper panel) and metamorphic (lower panel) Axolotl.
887 Reduction in limb regenerative capacity was observed for metamorphic animals. (n=15
888 for each group) **(b)**
889
890 **Figure 3. Effect of metamorphosis on bacterial diversity between neotenic and**
891 **metamorphic Axolotl.** Box plots illustrate the comparison of diversity indices; Observed
892 (a), Chao1 (b), Shannon (c) and Faith's Phylogenetic Diversity (PD) measures.
893
894 **Figure 4. Beta diversity analysis based on Bray-Curtis distance matrix showing**
895 **separation of neotenic and metamorphic bacterial communities**. Samples were
896 compared using PCO (a) and Canonical Analysis of Principal Coordinates (CAP) (b)
897 methods.
898

899 **Figure 5. Mean relative abundances of 16S rRNA sequences.** Phylum level relative
900 abundance as bar chart (a), genus level relative abundances shown as heatmap (Individual
901 taxa displayed if the its abundance in any sample ≥5%). Samples and bacterial taxa were
902 clustered using average linkage hierarchical clustering of a distance matrix based on
903 Bray–Curtis distance and taxa abundances, respectively. Samples from each group were
904 color coded on the column side bar as follows: Aqua samples (brown); samples from
905 neotenic Axolotl (light slate blue), metamorphic Axolotl (magenta) (b).
906
907 **Figure 6. Differentially enriched genus level taxa and indicator species in samples**
908 **from neotenic and metamorphic Axolotl**. The color scale bar indicates log2 fold
909 changes for absolute OTU abundances (DESeq2 analysis ($q$<0.01) (a), Bubble plot
910 showing indicator species. Only highly significant indicator values (IndVal>0.7, $q$<0.01)
911 are displayed. Size of bubble symbol is proportional to the mean relative abundance of
912 indicator OTUs and the color scale bar shows indicator value for each OTU (b).
913
914 **Figure 7. Venn diagrams showing the number of unique and shared OTUs.** Skin and
915 Aqua samples (a), and gut and fecal samples (b), collected from neotenic and
916 metamorphic Axolotls as indicated in the diagram.
917
918
919
920

Regeneration Experiments (n=30)

Neotenic Axolotls (n=48)

Untreated Axolotls. Maintained individually under constant diet; (6 weeks)

Randomization

Neotenic Axolotls n=9

Neotenic Axolotls n=9

Neotenic Axolotls n=9

Metamorphic Axolotls n=9

T4 hormone administration; maintained individually under constant diet; (6 weeks)

Rep1 Rep2 Rep3

Rep1 Rep2 Rep3

Pools (n=3) of Axolotl organs and stool

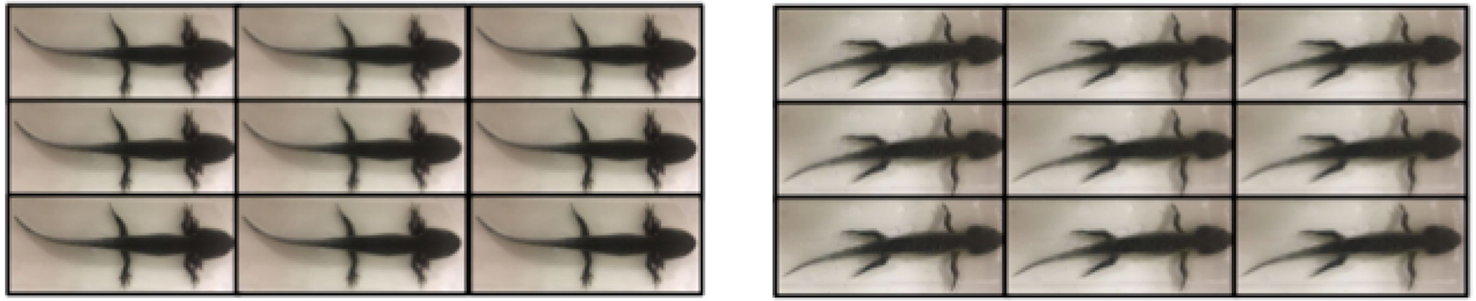

16S rRNA libraries, Sequencing on MiSeq and Data Analyses

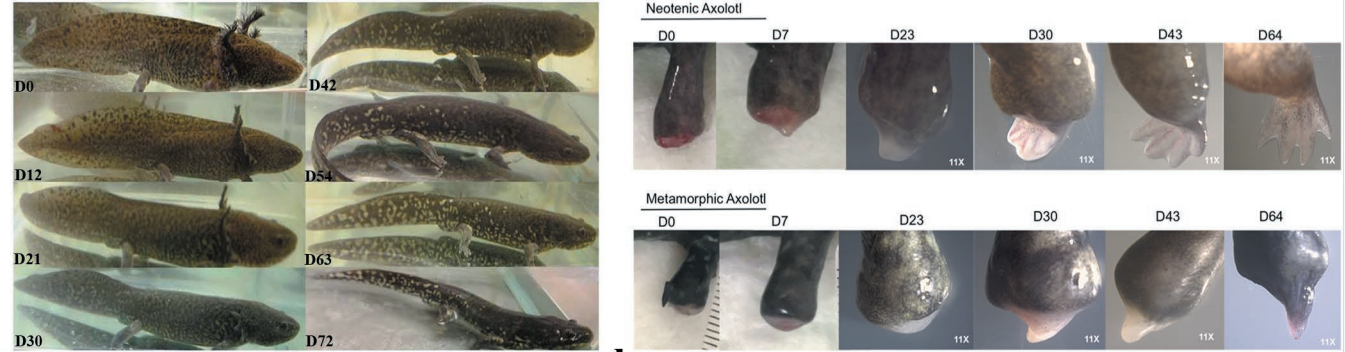
D0
D42
D12
D54
D21
D63
D30
D72
a
Neotenic Axolotl
D0
D7
D23
D30
D43
D64
11X
11X
11X
11X
Metamorphic Axolotl
D0
D7
D23
D30
D43
D64
11X
11X
11X
11X
b

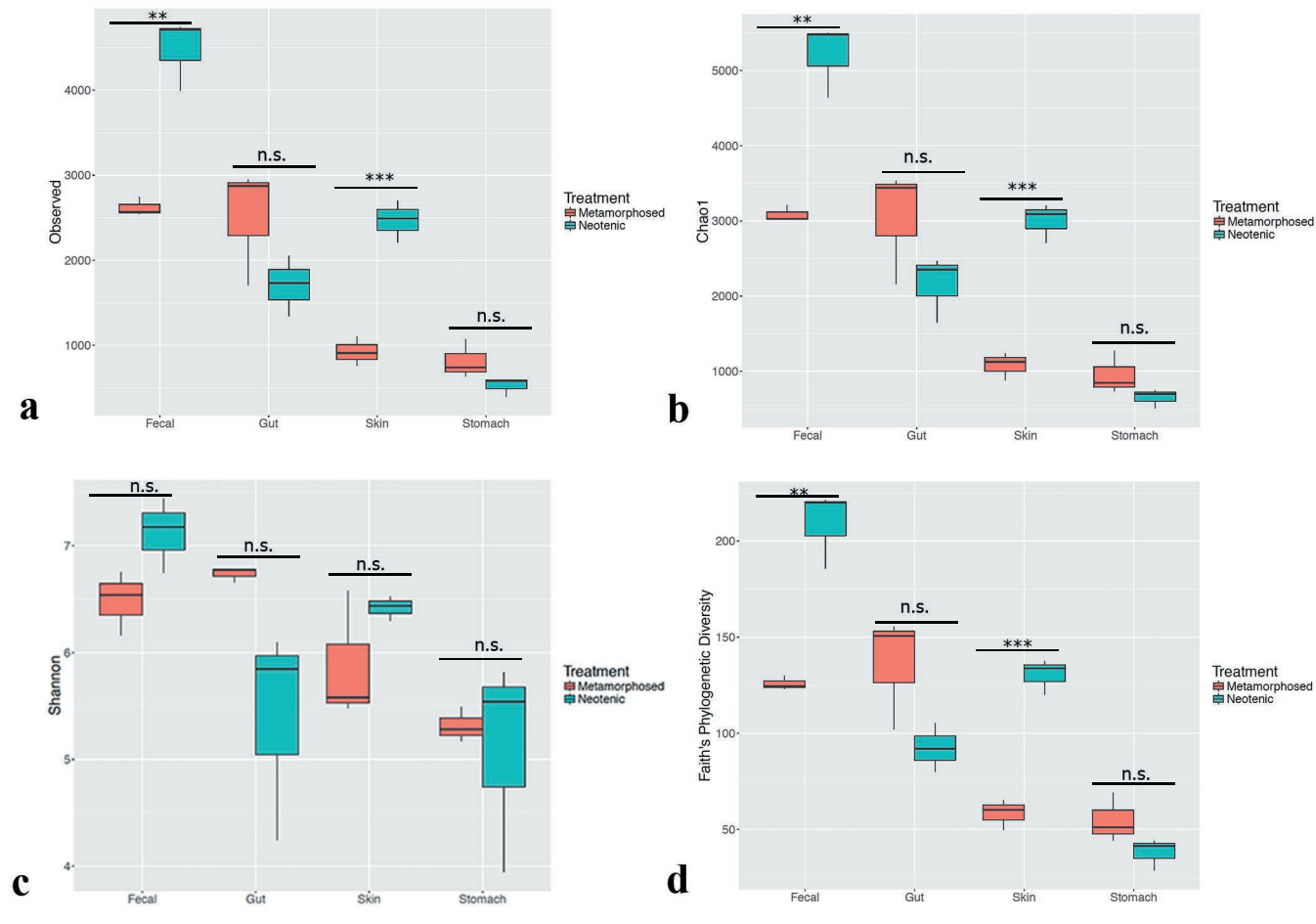
a
Observed
4000
3000
2000
1000
**
n.s.
***
n.s.
Fecal
Gut
Skin
Stomach
Treatment
Metamorphosed
Neotenic
b
Chao1
5000
4000
3000
2000
1000
**
n.s.
***
n.s.
Fecal
Gut
Skin
Stomach
Treatment
Metamorphosed
Neotenic
c
Shannon
7
6
5
4
n.s.
n.s.
n.s.
n.s.
Fecal
Gut
Skin
Stomach
Treatment
Metamorphosed
Neotenic
d
Faith's Phylogenetic Diversity
200
150
100
50
**
n.s.
***
n.s.
Fecal
Gut
Skin
Stomach
Treatment
Metamorphosed
Neotenic

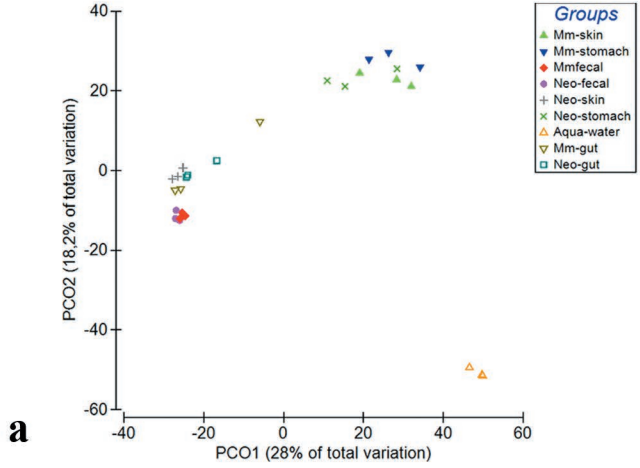
a
PCO2 (18,2% of total variation)
PCO1 (28% of total variation)
40
20
0
-20
-40
-60
-40
-20
0
20
40
60
Groups
Mm-skin
Mm-stomach
Mmfecal
Neo-fecal
Neo-skin
Neo-stomach
Aqua-water
Mm-gut
Neo-gut

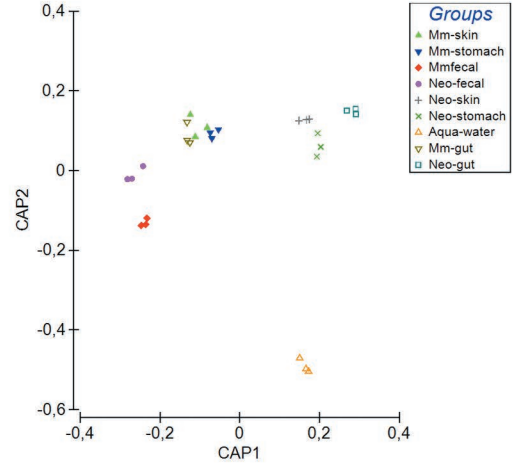
b
CAP2
CAP1
0,4
0,2
0
-0,2
-0,4
-0,6
-0,4
-0,2
0
0,2
0,4
Groups
Mm-skin
Mm-stomach
Mmfecal
Neo-fecal
Neo-skin
Neo-stomach
Aqua-water
Mm-gut
Neo-gut

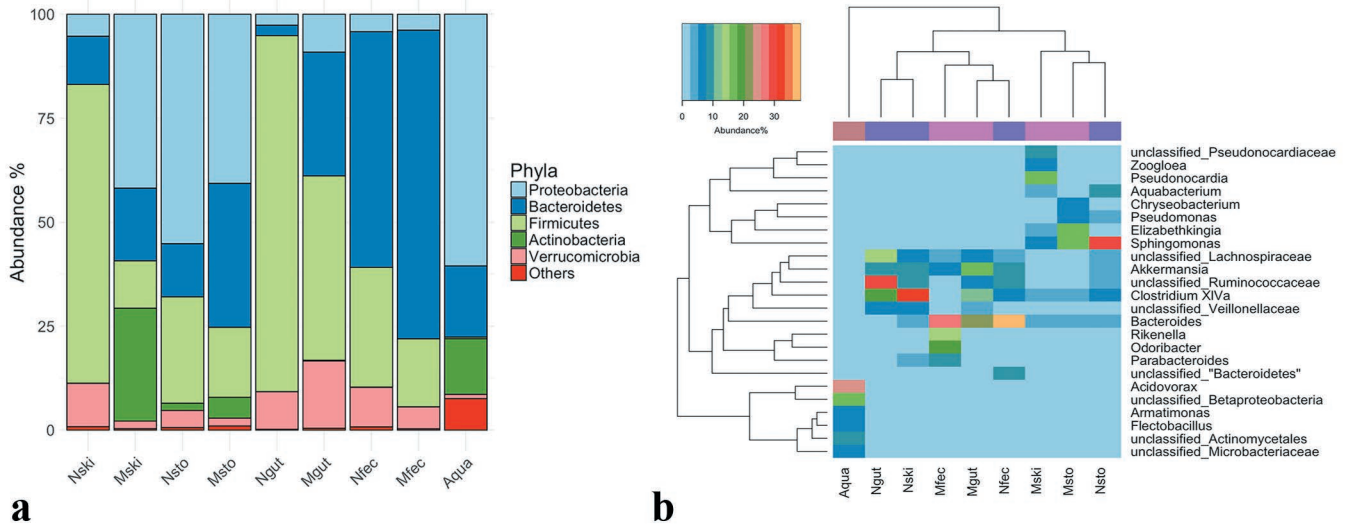
Abundance %
100
75
50
25
0
Nski
Mski
Nsto
Msto
Ngut
Mgut
Nfec
Mfec
Aqua
Phyla
Proteobacteria
Bacteroidetes
Firmicutes
Actinobacteria
Verrucomicrobia
Others
a
0
10
20
30
Abundance%
unclassified_Pseudonocardiaceae
Zoogloea
Pseudonocardia
Aquabacterium
Chryseobacterium
Pseudomonas
Elizabethkingia
Sphingomonas
unclassified_Lachnospiraceae
Akkermansia
unclassified_Ruminococcaceae
Clostridium XlVa
unclassified_Veillonellaceae
Bacteroides
Rikenella
Odoribacter
Parabacteroides
unclassified_"Bacteroidetes"
Acidovorax
unclassified_Betaproteobacteria
Armatimonas
Flectobacillus
unclassified_Actinomycetales
unclassified_Microbacteriaceae
Aqua
Ngut
Nski
Mfec
Mgut
Nfec
Mski
Msto
Nsto
b

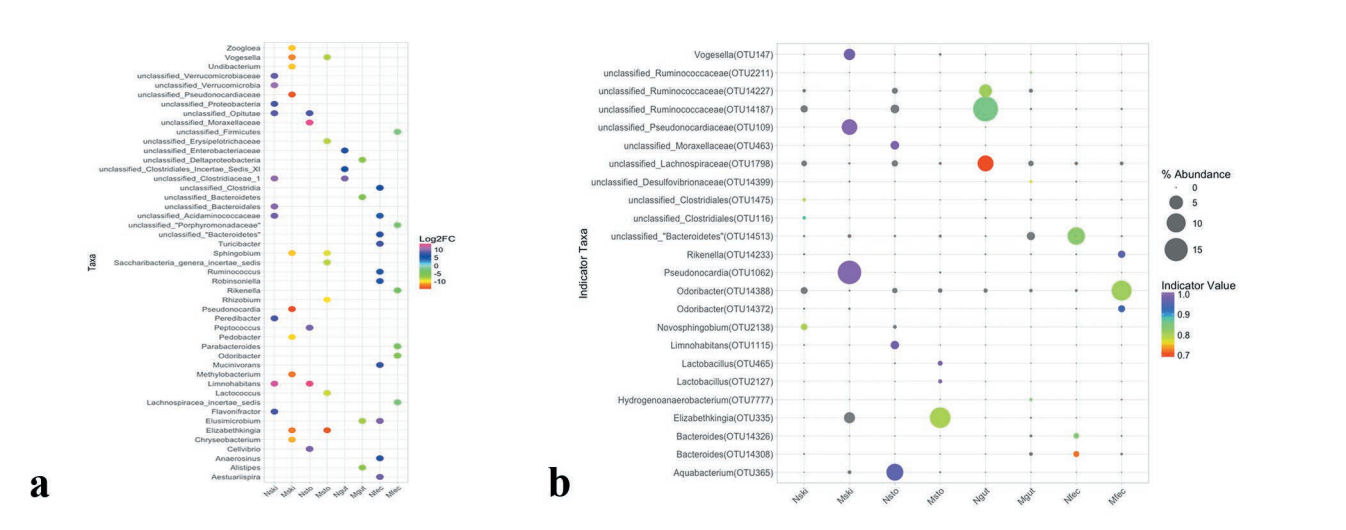
a
Taxa
Zoogloea
Vogesella
Undibacterium
unclassified_Verrucomicrobiaceae
unclassified_Verrucomicrobia
unclassified_Pseudonocardiaceae
unclassified_Proteobacteria
unclassified_Opitutae
unclassified_Moraxellaceae
unclassified_Firmicutes
unclassified_Erysipelotrichaceae
unclassified_Enterobacteriaceae
unclassified_Deltaproteobacteria
unclassified_Clostridiales_Incertae_Sedis_XI
unclassified_Clostridiaceae_1
unclassified_Clostridia
unclassified_Bacteroidetes
unclassified_Bacteroidales
unclassified_Acidaminococcaceae
unclassified_"Porphyromonadaceae"
unclassified_"Bacteroidetes"
Turicibacter
Sphingobium
Saccharibacteria_genera_incertae_sedis
Ruminococcus
Robinsoniella
Rikenella
Rhizobium
Pseudonocardia
Peredibacter
Peptococcus
Pedobacter
Parabacteroides
Odoribacter
Mucinivorans
Methylobacterium
Limnohabitans
Lactococcus
Lachnospiracea_incertae_sedis
Flavonifractor
Elusimicrobium
Elizabethkingia
Chryseobacterium
Cellvibrio
Anaerosinus
Alistipes
Aestuariispira
Log2FC
10
5
0
-5
-10
Nski
Mski
Nsto
Msto
Ngut
Mgut
Nfec
Mfec
b
Indicator Taxa
Vogesella(OTU147)
unclassified_Ruminococcaceae(OTU2211)
unclassified_Ruminococcaceae(OTU14227)
unclassified_Ruminococcaceae(OTU14187)
unclassified_Pseudonocardiaceae(OTU109)
unclassified_Moraxellaceae(OTU463)
unclassified_Lachnospiraceae(OTU1798)
unclassified_Desulfovibrionaceae(OTU14399)
unclassified_Clostridiales(OTU1475)
unclassified_Clostridiales(OTU116)
unclassified_"Bacteroidetes"(OTU14513)
Rikenella(OTU14233)
Pseudonocardia(OTU1062)
Odoribacter(OTU14388)
Odoribacter(OTU14372)
Novosphingobium(OTU2138)
Limnohabitans(OTU1115)
Lactobacillus(OTU465)
Lactobacillus(OTU2127)
Hydrogenoanaerobacterium(OTU7777)
Elizabethkingia(OTU335)
Bacteroides(OTU14326)
Bacteroides(OTU14308)
Aquabacterium(OTU365)
% Abundance
0
5
10
15
Indicator Value
1.0
0.9
0.8
0.7
Nski
Mski
Nsto
Msto
Ngut
Mgut
Nfec
Mfec

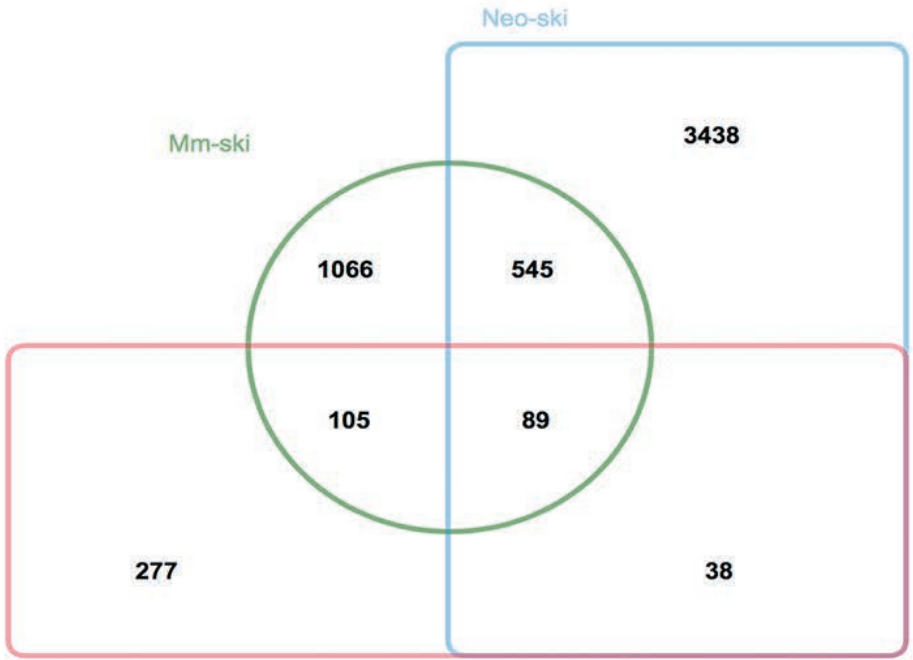
Neo-ski
Mm-ski
3438
1066
545
105
89
277
38
Aqua

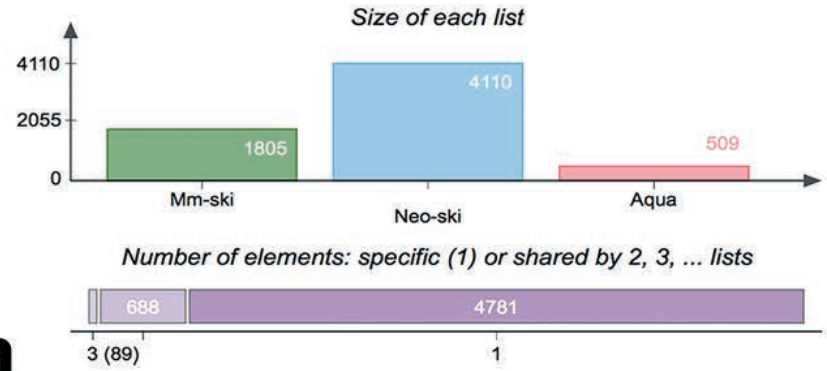
Size of each list
4110
2055
0
1805
4110
509
Mm-ski
Neo-ski
Aqua
Number of elements: specific (1) or shared by 2, 3, ... lists
688
4781
3 (89)
1

a

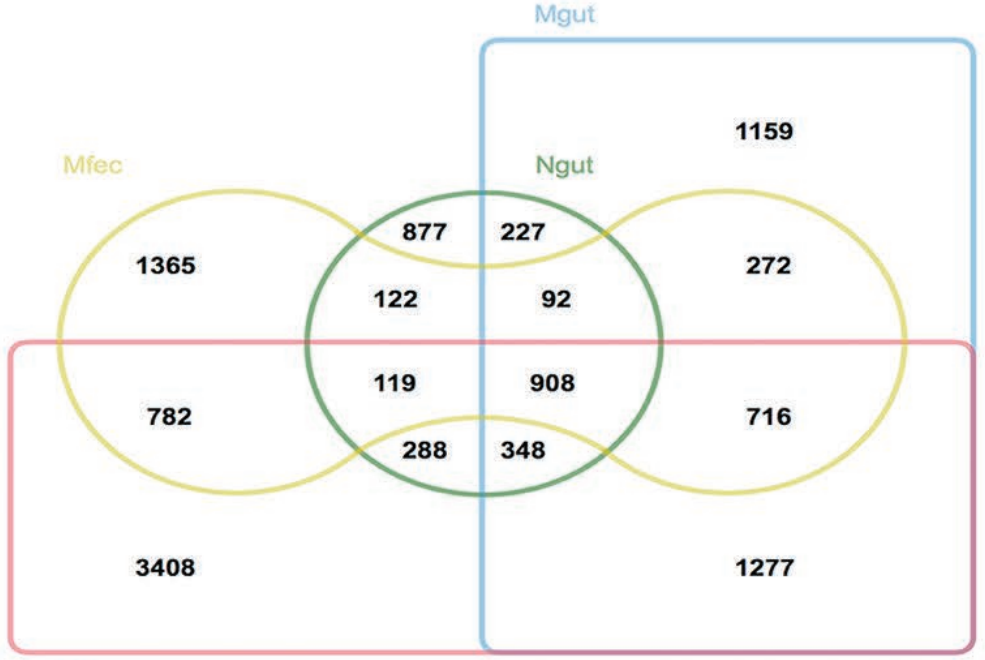
Mgut
1159
Mfec
Ngut
877
227
1365
272
122
92
119
908
782
716
288
348
3408
1277
Nfec

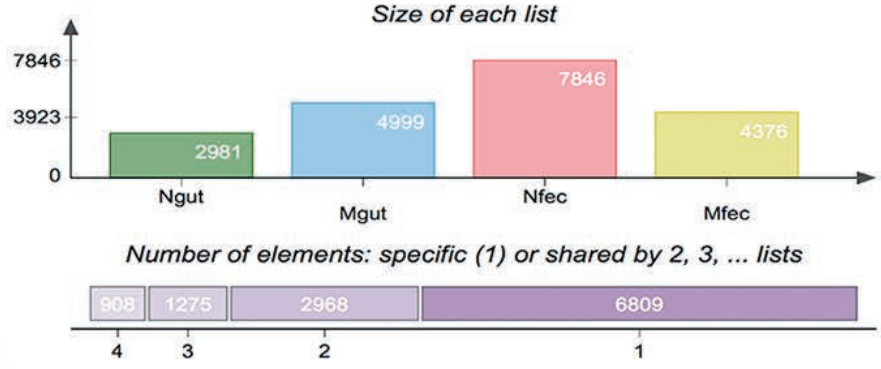
Size of each list
7846
3923
0
2981
4999
7846
4376
Ngut
Mgut
Nfec
Mfec
Number of elements: specific (1) or shared by 2, 3, ... lists
908
1275
2968
6809
4
3
2
1

b